Optimal Design to reduce Acoustic Noise in Interior Permanent Magnet Motor using Response Surface Methodology

Sang-Ho Lee, Suk-Hee Lee, Jung-Pyo Hong, Sang-Moon Hwang, Ji-Young Lee, and Young-Kyoun Kim

***Abstract*—This paper presents methods to reduce acoustic noise in interior permanent magnet (IPM) motor. Mechanical and magnetic sources are considered to reduce noise of the machine, and structural and electromagnetic designs are performed. In the structural design to reduce mechanical source, the resonant frequency of stator are moved to higher frequency for enhancement of stiffness and structural stability is also enhanced. Then, in the electromagnetic design to reduce magnetic source, the harmonic amplitude of normal force which affects stator pole is firstly reduced by using objective function of response surface methodology (RSM). In addition, second optimization for reduction of torque ripple is performed. The validity of the design procedures and objective function is confirmed with their calculated and experimental results.**

***Index Terms*— Acoustic noise, concentrated winding, design of experiment, interior permanent magnet, objective function, resonant frequency, stiffness, response surface methodology.**

I. Introduction

INTERIOR permanent magnet (IPM) motors have many advantages compared with surface permanent magnet (SPM) motors because IPM motors generate both magnetic torque and reluctance torque. However, regarding the noise and vibration, the IPM motors have more sources than SPM motors [1].

The harmonic of the forces which are divided into normal or tangential components is induced and the coincidence of the resonant frequencies of stator with any of the harmonic components of magnetic forces, especially normal force, will cause resonance resulting in vibration and noise [2].

Manuscript received June 30, 2006. This work was supported by grant No. RTIO04-01-03 from the Regional Technology Innovation Program of the Ministry of Commerce, Industry and Energy (MOCIE).

Sang-Ho LEE, Suk-Hee Lee, and Jung-Pyo HONG are with the Dept. of Electric Eng., Changwon National University, Changwon, 641-774, KOREA. (telephone: +82-55-262-5966, e-mail: tapaya@korea.com).

Sang-Moon Hwang is with the Dept. of Mechanical Eng., Pusan National University, Pusan, 609-735, KOREA. (telephone: +82-55-582-3104, e-mail: shwang@puasn.ac.kr).

Ji-Young LEE is with Transverse Flux Machine Research Group, Korea Electrotechnoloy Research Institude, Changwon, 641-120, KOREA. (telephone: +82-55-280-1156, e-mail: jylee@keri.re.kr).

Young-Kyoun KIM is with Power Electronics Group, Digital Appliance Business SAMSUNG ELECTRONICS CO.,LTD, 416, Maetan-3Dong, Suwon, 443-742, KOREA. (telephone: +82-31-218-5121, e-mail: youngkyoun.kim@samsung.com).

As one of the method of magnetic force calculation, equivalent magnetizing current (EMC) method uses magnetizing current which exists on element boundary and it can directly calculate the electromagnetic force which affects the surface of structure [3]. EMC only distributes on the element surface of different material because the interior magnetizing current in core is cancelled. The normal force is expressed as

$$f_n = \frac{1}{2}\left(H_{n1}B_{n1} - H_{t1}B_{t1}\right) - \frac{1}{2}\left(H_{n2}B_{n2} - H_{t2}B_{t2}\right) \quad (1)$$

where B_{n1}, B_{t1}, H_{n1}, and H_{t1} are the components in the air, B_{n2}, B_{t2}, H_{n2}, and H_{t2} are the components in the core.

In this paper, optimal design performs to reduce acoustic noise in IPM motor through structural and electromagnetic design. Especially, response surface methodology (RSM) is firstly applied in electromagnetic design and second optimization to reduce torque ripple is performed [4]-[5]. Accordingly, the validity of the design methodology to reduce noise is verified by comparison with calculated and experimental results.

II. Analysis of Prototype Model

As the brushless DC (BLDC) IPM motor with concentrated windings, specification of prototype is shown in Table I. The switch-on time is lagged behind 30^0 in electrical degree for back electromotive force (BEMF) in the no-load.

The configuration of noise experiment is shown as Fig. 1. Noise experiment is performed in the anechoic room where background noise is 41.0 dBA and measured 1m away from the motor by microphone. As a load of IPM motor, generator coupled with IPM motor produces the active power at the resistance.

TABLE I.
Specifications of Prototype

Contents	Values
Number of poles slots	4/6
Stack length (mm)	80.0
Rated current (A_{rms})	13.0
Number of turns per phase (turns)	65
Rated speed (rpm)	3000
Rated torque (Nm)	8.0
PWM frequency (kHz)	4.0

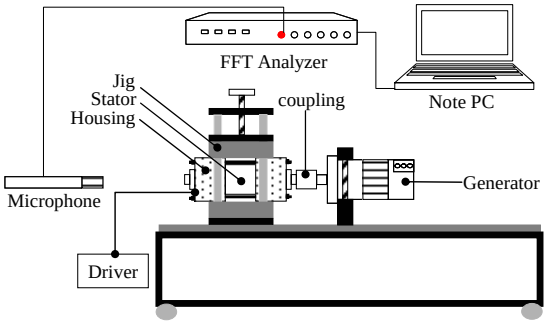

Fig. 1. Configuration of noise experiment.

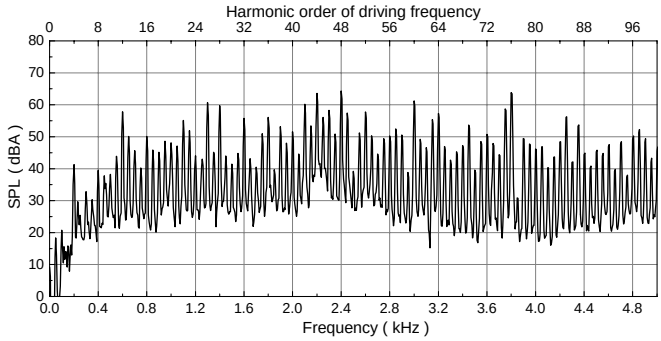

Fig. 2. Noise spectra of prototype (@ 3000 rpm, 8 Nm)

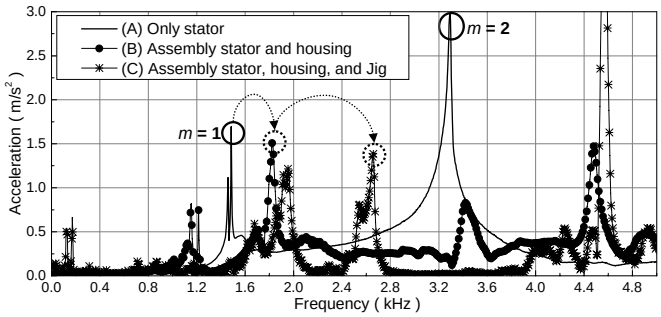

Fig. 3. The result of modal test for stator according to assembly condition.

TABLE II.
MECHANICAL MATERIAL PROPERTY OF STATOR

-	Mass density	Poisson's ratio	Elastic modulus
Values	7680 kg/m^3	0.3	200 GPa

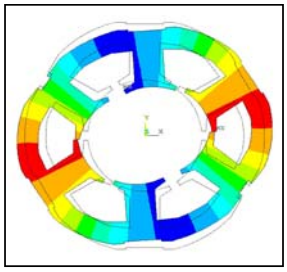

Fig. 4. Resonance mode m = 1 shape of stator by modal analysis (@ 1.5 kHz).

A. *Noise experiment*

The result of noise experiment prototype under 3000 rpm and 8 Nm is shown in Fig. 2. The noise spectra occur mostly four times of driving frequency and it corresponds with the harmonic component of normal force which affects stator pole.

The tendency of noise spectra in prototype has a great notation that the main noise between 2.0 and 2.8 kHz are generated by resonance and noise around 4 kHz are induced by pulse width modules (PWM) frequency.

B. *Modal test and analysis*

To verify noise source, modal test is performed for the element of motor and the result of modal test for stator is shown in Fig. 3. The frequencies of circumferential mode m = 1 of (A), (B), and (C) by assembly condition are 1.5, 1.8, and 2.6 kHz, respectively. The resonant frequency of stator is moved to higher frequency due to stiffness by assembly condition. Accordingly, the increase in resonant frequency of stator by assembly condition should be considered in noise experiment.

Considering mechanical material property which is expressed as table II, Fig. 4 shows resonance mode shape of circumferential mode m = 1 at 1.5 kHz obtained from the 2D FEM *Ansys.* And then, noise between 2.0 and 2.8 kHz mainly generates oval mode.

III. DESIGN METHODOLOGY

Design methodology to reduce acoustic noise is largely classified into two parts. First, structural design focuses on the reduction of the vibration by enhancing stiffness of stator. The quantities of vibration by changing the dimension of design variables are expressed by sound pressure levels (SPLs) which is calculated by using boundary element method (BEM) and then new stator shape is decided. Second, electromagnetic design concentrates on the harmonic reduction of normal force which is calculated by EMC.

A. *Structural design*

According to the change of each design variables, the variation of resonant frequency depending on the stator is analyzed. Link thickness (LT) and yoke thickness (YT) are main effective design variables to increase the resonant frequency in the design variables.

When the exciting force on the center of tooth surface is equal to 1 N, Fig. 5 shows the resonant frequency, vibration, and noise analysis results compared with prototype by changing LT and YT, respectively. According to the increase of the resonant frequency, quantities of vibration and noise are decreased because the kinetic energy of the air layer on the stator surface is the vibration energy of the stator [6]. Therefore, the reduction of vibration through the increase in LT and YT is necessary.

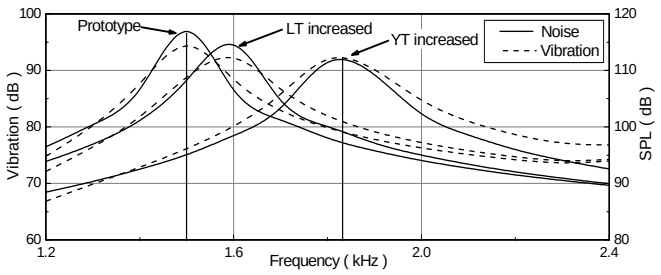

Fig. 5. Resonant frequency, vibration, and noise by changing LT and YT.

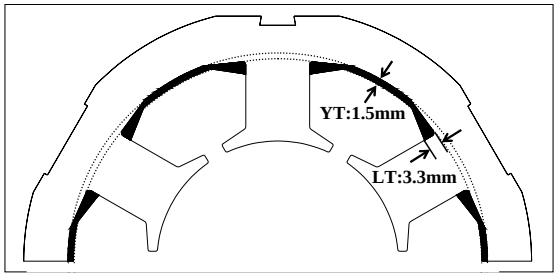

Fig. 6. The result of structural design.

Fig. 6 shows the shape and dimension, which is the result of structural design, compared with prototype when the constraint condition depends on possibility of windings. The black area means the expansion of core compared with prototype. The frequency of circumferential mode $m = 1$ of stator, it is the same condition such as (A) in Fig. 3, changes from 1.5 to 1.8 kHz. When the variation of mass by increasing the quantities of core compared with prototype is ignored, resonant frequency of stator is moved to higher frequency by the increase in stiffness and quantities of vibration which affects noise can be decreased.

Accordingly, structural design to reduce the acoustic noise in electric machines focuses on enhancement of the structural stiffness using LT and YT.

B. Electromagnetic design

Using the result of structural design, electromagnetic design to find optimal point reducing the harmonic of normal force which affects stator pole by RSM is firstly progressed. In addition, optimization to reduce torque ripple is secondly performed.

The harmonic of normal force is reduced by using an optimal design method. In the optimal design using RSM, objective functions and constraint condition are expressed as

$$\text{Objective function}: 10\log\sum 10^{\frac{F_n}{10}} \quad (2)$$

$$\text{Subject to}: \textit{Average torque} \geq 8.0\ Nm \quad (3)$$

Where F_n is the harmonic of normal force considering A-weighting in frequency weighting curves and weighting factor at the resonant frequency bands of stator [7].

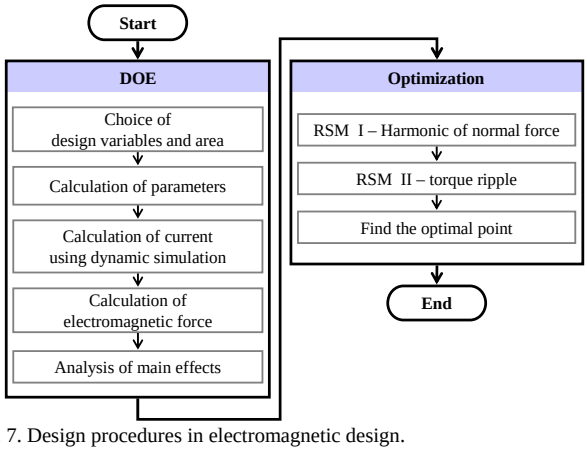

Fig. 7. Design procedures in electromagnetic design.

The design procedures of electromagnetic design are presented in Fig. 7. To consider operating condition of motor, parameters such as BEMF and inductance are calculated through FEA. In addition, current considering PWM frequency is calculated by duty ratio. Switch-on section is an important factor for distribution and harmonic components of normal force which affects stator pole. Yet, to analyze the results of objective function by design variables, the initial point of switch-on section, it lags behind 10^{0} in electrical degree for BEMF in the no-load, is fixed.

Fig. 8 shows the design variables, which are bridge width (BW), pole arc (PA), slot open (SO), and tooth height (TH). Full factorial design (FFD), which is required experiments 17 including central point, is used to find the main factors and design areas are shown in Table III. Main and interaction effects of BW, PA, and SO are significantly expressed from the result of DOE. Among those design variables, effective degree of PA and SO is higher than BW, therefore, PA and SO are firstly selected to reduce the harmonic of normal force in RSM.

Central composite design (CCD), which is required to conduct 9 experiments, is used to the response of each factor and design area of PA and SO based on the result of DOE shown in Table III. Initial optimal point considering constraint condition is shown in Fig. 9 and then PA and SO are 4.3 mm and 72 °, respectively.

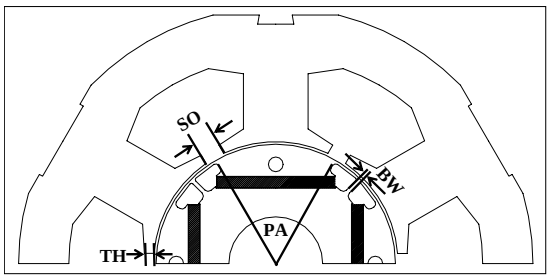

Fig. 8. Design variables in electromagnetic design.

TABLE III.
DESIGN VAIRALBES AND AREA IN ELECTROMAGNETIC DESIGN

	Design variables	Unit	Coded values				
			-1.682	1	0	1	1.682
DOE	BW	mm	-	0.5	2.5	4.5	-
	SO	mm	-	4.0	5.5	7.0	-
	TH	mm	-	1.5	2.5	3.5	-
	PA	°	-	45.0	65.0	75.0	-
RSM	SO	mm	3.89	4.35	5.45	6.55	7.00
	PA	°	50.08	53.4	61.4	69.4	72.71

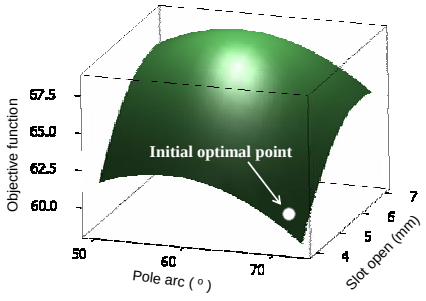

Fig. 9. Response surface of objective function.

Using the initial optimal point, second optimization to reduce torque ripple by changing BW is performed and then the values of objective function are also observed.

In the results by changing BW, the distribution of normal force which affects stator pole and torque of model having similar average torque compared with prototype are expressed in Fig. 10. Although the distribution of normal force is similar, torque ripple is decreased from 68.0 to 54.0 % and average torque is increased from 7.5 to 8.1 Nm. Therefore, BW is chosen as 2.5 mm in second optimization.

IV. Results and Disscusion

Fig. 11 and 12 show the comparisons of characteristics between prototype and optimized model (OPT), respectively. The distribution of normal force of OPT compared with prototype is more sinusoidal and peak values is lower than prototype but torque ripple of OPT is similar to prototype. Although the harmonic of torque ripple is lower than prototype, the harmonic amplitude of torque ripple generated by tangential force is very smaller than normal force. Accordingly, OPT only reduces the harmonic of normal force using the values of objective function.

Fig. 13 shows the noise experiment result measured by 1/3 octave band at the 3000 rpm and 8 Nm. Total SPLs of OPT compared with prototype are entirely reduced and the values of prototype and OPT are 76.5 and 71.4 dBA, respectively. The noise of prototype around PWM frequency is higher than OPT because inductance of OPT is higher than prototype due to the reduction of magnetic saturation by increasing pole arc.

V. Conclusion

This paper deals with optimal design to reduce acoustic noise in IPM motor using RSM. Acoustic noise of optimized model using proposed design procedures and objective function is reduced compared with prototype.

The structural design should focus on vibration reduction by increasing stiffness and stability of stator. In addition, the electromagnetic design should pay more attention to the harmonic reduction of normal force than one of tangential force in electric machine with high-power density such as IPM motor.

References

[1] Hong-Seok Ko, and Kwang-Joon Kim, “Characterization of Noise and Vibration Sources in Interior Permanent-Magnet Brushless DC Motors,” *IEEE Trans., Magn*., Vol. 40, No. 6, pp. 3482-3489, November, 2004.

[2] K. N. Srinivas, R. Arumugam, “Static and Dynamic Vibration Analyses of Switched Reluctance Motors Including Bearings, Housing, Rotor Dynamics, and Applied Loads,” *IEEE Trans., Magn.*, Vol. 40, No. 4, pp. 1911-1919, July 2004.

[3] G. Henneberger, P. K. Sattler, D. shen, “Nature of the equivalent magnetizing current for the force calculation,” *IEEE Trans., Magn.*, Vol. 28, No. 2, pp. 1068-1072, Mar. 1992.

[4] Sung-Il Kim, Jung-Pyo Hong, Young-Kyoun Kim, Hyuk Nam, Han-Ik Cho,"Optimal design of Slotless-Type PMLSM considering Multiple Response by Response Surface Methodology," *IEEE Trans. Magn*. Vol. 42, No. 4, pp.1219-1222, April, 2006.

[5] Kyung-Ho Ha, Yougn-Kyoun Kim, Geun-Ho Lee, and Jung-Pyo Hong, “Vibration Reduction of Switched Reluctance Motor by Experimental Transfer Function and Response Suerface Methodology,” *IEEE Trans., Magn.*, Vol. 40, No. 2, pp.577-580, Mar. 2004.

[6] Jacek F. Gieras, Chong Wang, Joseph Cho Lai, *Noise of Polyphase Electric Motors*, CRC press, 2006.

[7] Nau, S.L., Mello, H.G.G., "Acoustic noise in induction motors: causes and solutions," Petroleum and Chemical Industry Conference, 2000. *Industry Applications Society 47th Annual Conference Paper*, pp.253-263, 11-13, Sept, 2000.

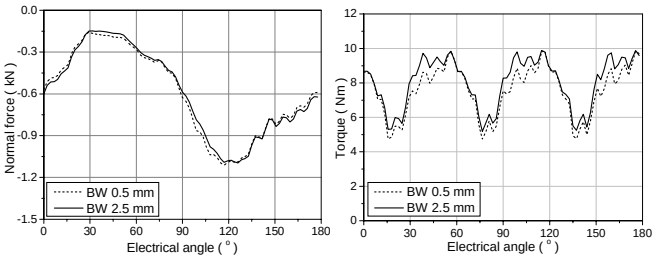

(a) Normal force (b) torque

Fig. 10. Characteristic according to change the BW (BW of prototype is 0.5mm).

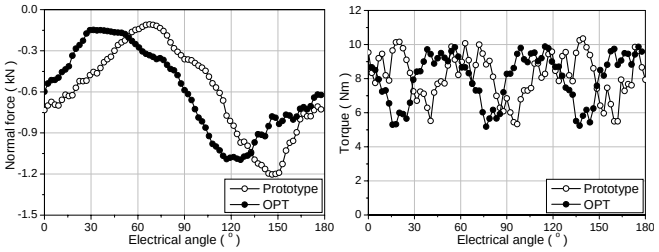

(a) Normal force (b) torque

Fig. 11. The distribution of normal force and torque.

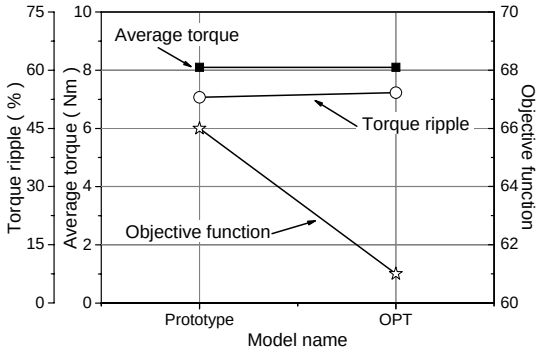

Fig. 12. The comparison between prototype and OPT characteristic.

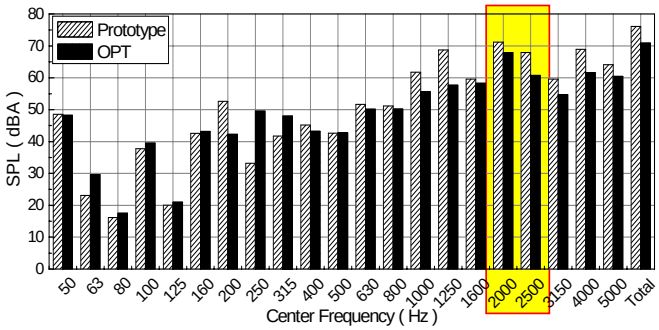

Fig. 13. The result of noise experiment (1/3 Octave band).

XVII International Conference on Electrical Machines

ICEM 2006

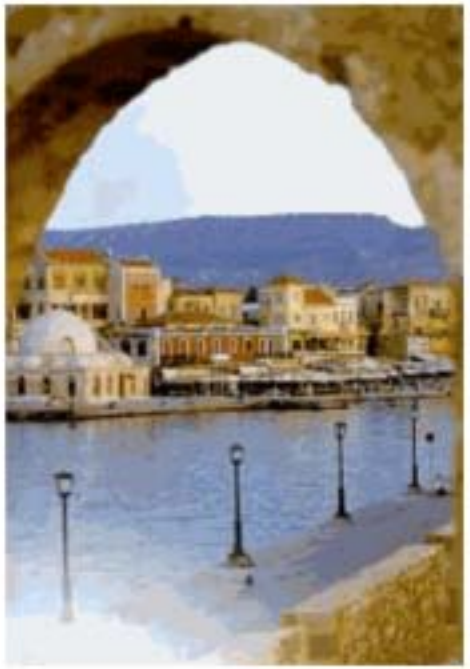

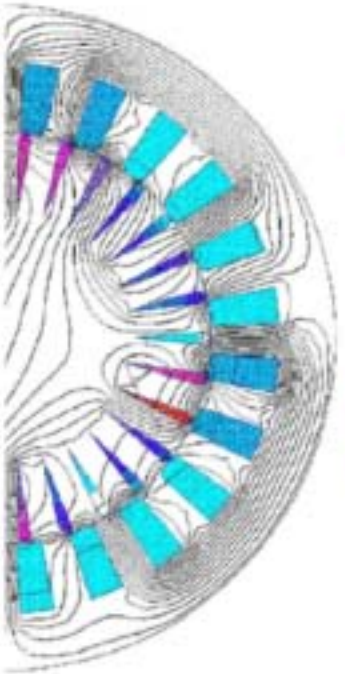

CONFERENCE PAPERS

Browse the ICEM 2006 Full Papers by:

- **Session**
- **Author**

September 2-5, 2006

Chania, Crete Island, Greece

Organising Institutions:

National Technical University of Athens

Technical University of Crete

Aristotle University of Thessaloniki

University of Patras

Democritus University of Thrace

15:30-16:40 POSTER (DIALOGUE) SESSION PSA1: PERMANENT MAGNET MACHINES

Saturday, September 2nd 2006

No	Ref	Paper title	Authors	Country of the corresponding author
PSA1-1	141	A Permanent Magnet Generator for Small Scale Wind Turbines	J.R. Bumby, N. Stannard and R. Martin	UK
PSA1-2	313	A Method for Dynamic Analysis of an Interior Permanent Magnet Motor Based on Nonlinear Magnetic Circuit	K. Nakamura, M. Ishihara, and O. Ichinokura	Japan
PSA1-3	163	High-speed permanent magnet generators design and testing	Yanush Danilevich, Victor Antipov	Russia
PSA1-4	180	An Attempt to Extend the Flux Weakening Range of a Single Stator Dual Rotor PM Machine	Imen Abdennadher, Ahmed Masmoudi and Ahmed Elantably	Tunisia
PSA1-5	234	Numerical design of DC brush motor with rare-earth magnets for ABS system including tolerances of input parameters	G. Ombach, J. Junak and A. Ackva	Germany
PSA1-6	244	A Stator Turn Fault Tolerant Strategy for Interior PM Synchronous Motor Drives in Safety Critical Applications	Youngkook Lee and T.G. Habetler	USA
PSA1-7	245	Comparative Evaluation of Axial Flux versus Radial Flux Permanent Magnet Synchronous Machines	M. Krishnamurthy, B. Fahimi and K. D. Oglesby	USA
PSA1-8	249	Design and Implementation of a Tubular Brushless DC Motor for Direct-Drive Applications	S.H. Mao, B.J. Lin, and M.C. Tsai	Taiwan
PSA1-9	250	Design of Interior Permanent Magnet Motors for Smoothening Back-EMF Waveform	H.S. Chen and M.C. Tsai	Taiwan
PSA1-10	251	Development of the Discontinuous Primary Permanent Magnet Linear Synchronous Motor	Kenji Suzuki, Yong-Jae Kim, Masaya Watada and Hideo Dohmeki	Japan
PSA1-11	254	Optimised design of concentrated winding PM brushless motors	A. Castagnini, P. Faure Ragani, G. Secondo	Italy
PSA1-12	266	Evaluation of Eddy Current Loss in Tubular Permanent Magnet Motors by Three-Dimensional Finite Element Analysis	J. Chai, J. Wang and D. Howe	UK
PSA1-13	267	Magnetic Field Distribution in Brushless Permanent Magnet AC Motors with Interior Permanent Magnets (IPM) and Slotted Stator	F. Poltschak, W.Amrhein	Austria
PSA1-14	274	A Brushless Permanent Magnet Motor with Hybrid Windings	M. C. Tsai and L. Y. Hsu	Taiwan
PSA1-15	276	Torque ripple reduction design of Multi-layer Interior Permanent Magnet Synchronour Motor by using Response Surface Methodology	Liang Fang, Soon-O Kwon, Peng Zhang, Jung-Pyo Hong	China
PSA1-16	311	Reluctance Network Analysis Model of a Permanent Magnet Generator Considering an Overhang Structure	K. Nakamura, M. Ishihara, and O. Ichinokura	Japan
PSA1-17	312	Multipolar Reluctance Generator Using Stator Core with Permanent Magnet	O. Ichinokura, T. Ono, T. Tashiro, K. Nakamura, and A. Takahashi	Japan
PSA1-18	346	Distribution, coil-span and winding factors for AFPM with concentrated windings	S. E. Skaar, Ø. Krøvel, R. Nilssen	Norway
PSA1-20	284	Application of a Toroidal Harmonic Expansion for Computing the Magnetic Field from a Balanced 6-Pole Permanent-Magnet Motor	J. Selvaggi, S. Salon, O. Kwon, and M.V.K. Chari	USA

11:40-13:20 ORAL SESSION OTM4: TESTING, MEASUREMENTS, ACOUSTIC NOISE AND VIBRATION ASPECTS

Tuesday, September 5th 2006

Ariadne Room

No	Ref	Paper title	Authors	Country of the corresponding author
OTM4-1	320	Testing of Electric Machines with a Dedicated System for Data Acquisition and Processing	Voicu Groza, Marius Biriescu, Vladimir Crețu, Gheorghe Liuba, Marțian Moț , Gheorghe Madescu	Romania
OTM4-2	197	The increase of the magnetic noise of induction motors due to the low order excitation modes generated by the rotor ecoentricity	S.L. Nau, R. Beck, H.L.V. dos Santos, N. Sadowski, R. Carlson	Brazil
OTM4-3	452	Monitoring of Induction Motors Rotor Faults by non invasive sensors	A. Bellini, C. Concari, G. Franceschini, C. Tassoni, A. Toscani	Italy
OTM4-4	505	Acoustic Noise and Displacement Analysis of a 3-phase Transformer Core Under Sinusoidal and PWM Excitations	X G Yao, Thant P P Phway, A J Moses, F Anayi	UK
OTM4-5	546	Optimal Design to reduce Acoustic Noise in Interior Permanent Magnet Motor using Response Surface Methodology	Sang-Ho Lee, Suk-Hee Lee, Jung-Pyo Hong, Sang-Moon Hwang, Ji-Young Lee, and Young-Kyoun Kim	Korea

15:30-16:40 POSTER (DIALOGUE) SESSION PSA1: PERMANENT MAGNET MACHINES

Saturday, September 2nd 2006

No	Ref	Paper title	Authors	Country of the corresponding author
PSA1-1	141	A Permanent Magnet Generator for Small Scale Wind Turbines	J.R. Bumby, N. Stannard and R. Martin	UK
PSA1-2	313	A Method for Dynamic Analysis of an Interior Permanent Magnet Motor Based on Nonlinear Magnetic Circuit	K. Nakamura, M. Ishihara, and O. Ichinokura	Japan
PSA1-3	163	High-speed permanent magnet generators design and testing	Yanush Danilevich, Victor Antipov	Russia
PSA1-4	180	An Attempt to Extend the Flux Weakening Range of a Single Stator Dual Rotor PM Machine	Imen Abdennadher, Ahmed Masmoudi and Ahmed Elantably	Tunisia
PSA1-5	234	Numerical design of DC brush motor with rare-earth magnets for ABS system including tolerances of input parameters	G. Ombach, J. Junak and A. Ackva	Germany
PSA1-6	244	A Stator Turn Fault Tolerant Strategy for Interior PM Synchronous Motor Drives in Safety Critical Applications	Youngkook Lee and T.G. Habetler	USA
PSA1-7	245	Comparative Evaluation of Axial Flux versus Radial Flux Permanent Magnet Synchronous Machines	M. Krishnamurthy, B. Fahimi and K. D. Oglesby	USA
PSA1-8	249	Design and Implementation of a Tubular Brushless DC Motor for Direct-Drive Applications	S.H. Mao, B.J. Lin, and M.C. Tsai	Taiwan
PSA1-9	250	Design of Interior Permanent Magnet Motors for Smoothening Back-EMF Waveform	H.S. Chen and M.C. Tsai	Taiwan
PSA1-10	251	Development of the Discontinuous Primary Permanent Magnet Linear Synchronous Motor	Kenji Suzuki, Yong-Jae Kim, Masaya Watada and Hideo Dohmeki	Japan
PSA1-11	254	Optimised design of concentrated winding PM brushless motors	A. Castagnini, P. Faure Ragani, G. Secondo	Italy
PSA1-12	266	Evaluation of Eddy Current Loss in Tubular Permanent Magnet Motors by Three-Dimensional Finite Element Analysis	J. Chai, J. Wang and D. Howe	UK
PSA1-13	267	Magnetic Field Distribution in Brushless Permanent Magnet AC Motors with Interior Permanent Magnets (IPM) and Slotted Stator	F. Poltschak, W.Amrhein	Austria
PSA1-14	274	A Brushless Permanent Magnet Motor with Hybrid Windings	M. C. Tsai and L. Y. Hsu	Taiwan
PSA1-15	276	Torque ripple reduction design of Multi-layer Interior Permanent Magnet Synchronour Motor by using Response Surface Methodology	Liang Fang, Soon-O Kwon, Peng Zhang, Jung-Pyo Hong	China
PSA1-16	311	Reluctance Network Analysis Model of a Permanent Magnet Generator Considering an Overhang Structure	K. Nakamura, M. Ishihara, and O. Ichinokura	Japan
PSA1-17	312	Multipolar Reluctance Generator Using Stator Core with Permanent Magnet	O. Ichinokura, T. Ono, T. Tashiro, K. Nakamura, and A. Takahashi	Japan
PSA1-18	346	Distribution, coil-span and winding factors for AFPM with concentrated windings	S. E. Skaar, Ø. Krøvel, R. Nilssen	Norway
PSA1-20	284	Application of a Toroidal Harmonic Expansion for Computing the Magnetic Field from a Balanced 6-Pole Permanent-Magnet Motor	J. Selvaggi, S. Salon, O. Kwon, and M.V.K. Chari	USA

10:20-11:30 POSTER (DIALOGUE) SESSION PTM2: DRIVES OF SYNCHRONOUS, PM AND DC MACHINES

Tuesday, September 5th 2006

No	Ref	Paper title	Authors	Country of the corresponding author
PTM2-1	526	Operational Behaviour of Industrial DC Drives in Paper Machines in Relation to Elastic Shafts Characteristics	C. Michael, A. Safacas	Greece
PTM2-3	344	Accurate Torque Control of VSI Fed Synchronous Machine Under Normal or Fault Conditions Using Discrete Modelling of Airgap Flux	M. Bekemans, F. Labrique, E. Matagne	Belgium
PTM2-4	702	Brushless, Self-Excited Synchronous Field-Winding Machine for Variable-Speed Drive Applications	Alexander Rovnan, Heath Hofmann	USA
PTM2-5	128	The New Methodology Of The Power Loss Calculation Under Deformed Flux Conditions	Z. Gmyrek, A. Boglietti, A. Cavagnino	Poland
PTM2-6	415	AC High Dynamometer for testing motor drive system	Gildong Kim, Hanmin Lee, Sehchan Oh, Sunghyuk Park, Changmu Lee	Korea
PTM2-7	341	Fast Prototyping of Vector Controllers for Interior PM Synchronous Motors	M. Tursini, A. Scotti, D. D'Antonio, and E. Chiricozzi	Italy
PTM2-8	379	Current Waveform Analysis of PWM Inverter-Fed Permanent Magnet Synchronous Machine Accounting for Cross-Magnetization	M. Kimura, K. Ide, H. Mikami	Japan
PTM2-9	342	Sensorless Control of PM Synchronous Motors with Luenberger Observer: Theoretical Issues and Implementation Results	M. Tursini, A. Scafati, R. Petrella	Italy
PTM2-10	460	Speed Control of Permanent Magnet Synchronous Motors by Current Vector Control	P. Fernandez, J. A. Goemes and A. M. Iraolagoitia	Spain
PTM2-11	626	Line-Start Permanent-Magnet Chemical Pump Drives	A.C.Smith and E.Peralta Sanchez	UK
PTM2-12	237	Versatile High Torque Direct Drive with PM-Excitation and Duplex Stator Arrangement	W.-R. Canders, H. Mosebach, M. R. Rezaei	Germany
PTM2-13	257	A Novel Drive Strategy for Vibration Suppression in Permanent Magnet Brushless DC Motor	Tao. Sun, Gen-Ho Lee, Jeng-Pyo Hong	Korea
PTM2-14	129	Implementation of an active converter for high quality dc drive performance	N.N. Barsoum, S.K. Wong	Malaysia
PTM2-15	155	Controlled DC Electric Drive Based on Stochastic Calculation Techniques	Achmad Alyan and Raul Rabinovici	Israel
PTM2-16	307	Determination of the Optimum Power Factor and Efficiency of a Characteristic DC Drive System via Simulation	K. Georgakas, A. Safacas, I. Georgakopoulos	Greece
PTM2-17	440	Optimal Integral State Feedback controller for a DC motor	H. Delavari, GH. Alizadh, M.Sharifian,	Iran
PTM2-18	255	Simplified sensorless control technique for wound rotor synchronous motor	F. Chabour, J. P. Vilain, P. Macret, P. Masson, L. Kobylansky	France